PHYSICAL REVIEW D **91,** 083005 (2015)

Post-Planck dark energy constraints

Dhiraj Kumar Hazra[*]
Asia Pacific Center for Theoretical Physics, Pohang, Gyeongbuk 790-784, Korea

Subhabrata Majumdar[†]
Tata Institute for Fundamental Research, Mumbai 400005, India

Supratik Pal[‡]
Physics and Applied Mathematics Unit, Indian Statistical Institute, Kolkata 700108, India

Sudhakar Panda[§]
Institute of Physics, Sachivalaya Marg, Bhubaneswar 751005, India

Anjan A. Sen[¶]
Center For Theoretical Physics, Jamia Millia Islamia, New Delhi 110025, India
(Received 29 December 2014; published 13 April 2015)

We constrain plausible dark energy models using the recently published cosmic microwave background (CMB) temperature anisotropy data from Planck together with WMAP9 low-ℓ polarization data and the data from low redshift surveys. To circumvent the limitations of any particular equation of state toward describing all existing dark energy models, we work with three different equations of state covering a wider class of dark energy models and hence provide more robust and generic constraints on the dark energy behavior. We show that a possible tension exists between constraints from CMB and non-CMB observations when one allows for both phantom and nonphantom behavior for the dark energy. Further, we reconstruct the equation of state of dark energy as a function of redshift using the combined CMB and non-CMB data and show that cosmological constant behavior is disallowed at the 68.3% confidence level. A fully nonphantom history is also disallowed at the 68.3% confidence level, and a considerable fine-tuning is also needed to keep it inside the 95.5% confidence limit. This result might motivate one to construct phantom models for dark energy, which may be achievable in the presence of higher derivative operators as in string theory. However, for a theoretical model that allows only nonphantom behavior, both CMB and non-CMB data sets agree on the dark energy constraint with the mean equation of state being very close to the cosmological constant.

DOI: 10.1103/PhysRevD.91.083005 PACS numbers: 95.36.+x, 98.80.-k

I. INTRODUCTION

It is now established by a range of cosmological observations, that our Universe is going through a late time accelerated expansion phase. To explain such an accelerating universe, either one needs to add an additional component, called dark energy, in the energy budget of the Universe that necessarily has a negative pressure causing an overall repulsive behavior of gravity at large cosmological scales (see [1] for some excellent reviews) or one has to modify Einstein's general relativity. Unfortunately, while candidates for dark energy have been proposed, its exact nature remains unknown. Alternatively, satisfactory modifications of general relativity consistent with gravitational physics at astrophysical scales are also lacking.

Observational data are not yet sufficient to tightly constrain the nature of dark energy, specifically its equation of state. One would also like to know whether this equation of state satisfies the weak energy condition (WEC) such that it dilutes with the cosmological expansion, or whether it violates the WEC and behaves like some mysterious form of phantom energy with its energy density increasing with time and possibly leading to a future singularity.

The majority of the current and future cosmological observational programs are dedicated to finding answers to these pertinent questions. These include, among others, (i) the reconstruction of the Hubble diagram using Supernova Type-Ia as a standard candle [2], (ii) measuring fluctuations in the temperature of the cosmic microwave background (CMB) radiation [3,4], or (iii) measuring the acoustic oscillations in the matter power spectrum through large scale structure surveys [5].

[*]dhiraj@apctp.org
[†]subha@tifr.res.in
[‡]supratik@isical.ac.in
[§]panda@iopb.res.in
[¶]aasen@jmi.ac.in

The simplest example for dark energy is the cosmological constant (Λ), which provides a fixed constant equation of state of dark energy [Pressure $(p) \equiv -$energy density (ρ)]. The concordance ΛCDM model is consistent with most of the cosmological observations. However, underlying theoretical issues, such as fine-tuning as well as cosmic coincidence problems, have motivated people to explore beyond the cosmological constant, the natural alternatives being scalar field models. A variety of such scalar field models, including string theory embeddings for a positive cosmological constant [6], quintessence [7], k essence [8], phantom fields [9], and tachyons [10], have been proposed. Other than scalar field models, a barotropic fluid with an equation of state $p(\rho)$, such as the generalized Chaplygin gas (GCG) and its various generalizations [11,12], have also been considered for dark energy model building.

Present cosmological observations provide us with a precise description of the Universe and impose tight constraints on the standard cosmological model. However, given the proliferation of dark energy models in the literature, it is impractical to confront each model with the observational data. Rather one needs to look for generic features of dark energy that are present in a large class of models and then to confront these features with the observational results. The most popular way of doing this is to assume a parametrization for the dark energy equation of state w as a function of redshift, z, or the scale factor, a. One such widely used parametrization is the Chevallier-Polarski-Linder (CPL) parametrization first discussed in [13] and later in [14]. This particular parametrization uses a linear dependence of the equation of state on the scale factor and has been used by almost all recent cosmological observations to put constraints on w. However, it may not correctly represent models with more complicated a dependence at slightly higher redshifts where a dark energy contribution might still be non-negligible. Hence, constraining dark energy behavior using *only* the CPL parametrization might give biased or even incorrect conclusions.

Given the fact that Planck [4], in combination with non-CMB observations like SN-Ia, baryon acoustic oscillations (BAO), and hubble space telescope (HST), has measured the cosmological content of the Universe with unprecedented accuracy, it is now interesting to investigate how different parametrizations of the dark energy equation of state can result in different constraints on dark energy behavior when confronted with the observational data. We can, now, address the following: Are conclusions regarding the nature of dark energy borne out of observational data biased by our choice of parametrization? Or does a general pattern exist in the dark energy behavior that is always true even if we consider different parametrizations for the dark energy equation of state?

In this paper, we investigate these issues by considering two other parametrizations for the dark energy equation of state together with the CPL parametrization. The first was proposed by Scherrer and Sen (SS) [15], and it represents the slow-roll thawing class of canonical scalar field models having an equation of state that varies very close to the $w = -1$ irrespective of the form of the potential. The second parametrization that we consider was proposed by Bento, Bertolami, and Sen [11], subsequently was discussed [16–19] for more general parameter ranges in [12], and is known as the GCG parametrization. In Section 2, we describe the details of these two parametrizations.

For each of these cases, we investigate the departure of the cosmological parameters from the ΛCDM best-fit values. Note that the CPL parametrization has already been discussed in the Planck analysis [20]. However, our analysis, apart from showing a consistency check with Planck results, provides some new facts and highlights a moderate tension between CMB and non-CMB observations. Using the CMB, non-CMB, and combined data of both, we demonstrate this tension between high-redshift and low-redshift measurements for models allowing phantom behavior. Moreover from the combined analysis, using the correlation between the equation of state parameters we reconstruct the allowed range of dark energy evolution with redshift and address the stand of phantom and nonphantom models in the allowed band. In particular, we show that, once we disallow phantom behavior, w is extremely close to the cosmological constant.

At this point it should be noted that, as an alternative approach, model independent reconstructions of the expansion history [i.e., the Hubble parameter $h(z)$] have been carried out before [21,22], from which the equation of state can also be reconstructed. Also note that certain parametrization of the dark energy equation of state may "artificially" limit the properties of dark energy from explaining a few effects, such as the recent slowdown of cosmic acceleration [23]. To overcome such biases, in this current work, we use three different kinds of dark energy parametrizations in order to cover a broad spectrum of dark energy behavior. We constrain the nature of dark energy using CMB and non-CMB surveys, taken individually as well as jointly (see [24] for some recent works on dark energy constraint after Planck).

The paper is organized as follows. In Section II, we briefly discuss the three dark energy parametrizations that we use in this paper; in Section III, we describe the different observational data sets that we use to constrain the dark energy evolution. We present the results in Section IV, and in Section V, we summarize.

II. DARK ENERGY PARAMETRIZATIONS

A. CPL parametrization

This parametrization dictates that the equation of state of dark energy has the following form:

$$w(a) = w_0 + w_a(1-a) = w_0 + w_a\frac{z}{1+z}, \qquad (1)$$

where w_0 and w_a are the two parameters in the model. They represent the equation of state at present ($a = 1$) and its variation with respect to scale factor (or redshift). From the infinite past till the present time, the equation of state is bounded between $w_0 + w_a$ and w_0. The dark energy density, in this case, evolves as

$$\rho_{DE} \propto a^{-3(1+w_0+w_a)} e^{-3w_a(1-a)}. \quad (2)$$

This equation of state remarkably fits a wide range of scalar field dark energy models including the supergravity-inspired supergravity dark energy models. The CPL parametrization is most commonly used in the literature to study the nature of dark energy. An outcome of the specific form of this parametrization is that, for $w_0 \geq -1$ and $w_a > 0$, the dark energy remains nonphantom in nature throughout the cosmological evolution; otherwise it shows phantom behavior at some point in time.

B. SS parametrization

This parametrization proposed in [15] is for the slow-roll "thawing" class of scalar field models having a canonical kinetic energy term. The main motivation for this parametrization was to look for a unique dark energy evolution for scalar field models that are constrained to evolve very close to the cosmological constant ($w = -1$). Since similar situations also arise in inflationary scenarios in the early universe, one assumes the same slow-roll conditions on the scalar field potentials as used in inflation. However, unlike the inflationary epoch, the evolution of the Universe significantly differs due to the presence of the large matter content in the late universe; still it can be shown that (i) under the assumption of the two slow-roll conditions and that (ii) the scalar field is initially frozen at $w = -1$ due to large Hubble damping (termed "thawing class"), one gets a unique form for the dark energy equation of state irrespective of its potential. The form of this equation of state, for a universe with flat spatial hypersurface, is given by

$$w(a) = (1 + w_0)\left[\sqrt{1 + (\Omega_{DE}^{-1} - 1)a^{-3}} - (\Omega_{DE}^{-1} - 1)a^{-3}\tanh^{-1}\frac{1}{\sqrt{1 + (\Omega_{DE}^{-1} - 1)a^{-3}}}\right]^2 \times \left[\frac{1}{\sqrt{\Omega_{DE}}} - \left(\frac{1}{\Omega_{DE}} - 1\right)\tanh^{-1}\sqrt{\Omega_{DE}}\right]^{-2} - 1. \quad (3)$$

Note that SS has one model parameter, w_0, which represents its value at the present epoch together with the general cosmological parameter Ω_{DE} representing the present day dark energy density. The energy density of this model of dark energy can be calculated analytically using the Friedmann equations that have been used in our analysis. Subsequently, the idea was also extended to phantom-type scalar field models with a negative kinetic energy term [25], for the tachyon-type scalar field models [26] having DBI-type kinetic energy term [27] and also for the axionic quintessence model in string theory [28].

C. GCG parametrization

The Chaplygin gas (CG) equation of state was first discussed in the cosmological context in [29] and is described by

$$p = -\frac{c}{\rho}, \quad (4)$$

where c is an arbitrary constant and p and ρ represent the pressure and energy density of the CG fluid. Subsequently, this equation of state was generalized in [11] and in [30] as

$$p = -\frac{c}{\rho^\alpha}, \quad (5)$$

where α is a constant within the range $0 \leq \alpha \leq 1$. This form is known as the GCG equation of state. In a later work [12] the parameter range $\alpha < 0$ was considered to describe diverse cosmological behaviors. Assuming a spatially flat universe the equation of state can be represented as

$$w(a) = -\frac{A}{A + (1 - A)a^{-3(1+\alpha)}}, \quad (6)$$

where $A = c/\rho_{GCG}^{1+\alpha}$. The GCG parametrization contains two model parameters, e.g., A and α.

It is easy to check that the present equation of state $w(0) = -A$. For $(1 + \alpha) > 0$, $w(a)$ behaves like a dust in the past, evolves toward negative values, and becomes $w = -1$ in the asymptotic future. This is similar to "tracker/freezer" behavior for a scalar field where it tracks the background matter in the past, and in the late time behaves like a dark energy with a negative equation of state. For $(1 + \alpha) < 0$, the opposite happens. In this case the $w(a)$ is frozen to $w = -1$ in the past, and it slowly evolves toward higher values and eventually behaves like a dust in the future. This behavior is similar to the thawing class of scalar field models. Moreover, in this case, the late time acceleration is a transient phenomenon as the acceleration slows down eventually and the Universe enters again a dust regime. For both thawing or freezing kinds of behaviors, the transition to/from $w = -1$ depends on the value of α.

We shall consider both $1+\alpha>0$ and $1+\alpha<0$ to consider freezing- as well as thawing-type behaviors. However, we restrict $0<A<1$ only since for $A>1$ singularity appears at finite past. As a consequence, this model is restricted to probe dark energy behavior for nonphantom cases only, a feature that is also true for scalar field models with positive kinetic energy. We have also chosen $-3\leq\alpha\leq 3$. From Eq. (6) a large negative value of α suggests that the equation of state will converge to the cosmological constant faster in the past, and hence α will have no lower bounds even if we allow for lower values of α.[1] The upper limit of α is chosen such that the tail of the marginalized probability distribution function converges before the upper limit. Recently, this parametrization has been used [31] to study the Bayesian evidence for the thawing/freezing class of the dark energy models using different observational results including WMAP-7 results.

The three parametrizations for the dark energy equation of state that we considered complement each other to describe a broad spectrum for dark energy behavior. CPL with a linear dependence in scale factor takes care of the dark energy evolution around present day, GCG takes care of the thawing and tracking nature of the dark energy, and SS describes models that are very close to ΛCDM but not exactly ΛCDM. GCG in particular is a nonphantom model by definition and can be used to see whether a nonphantom theoretical model is consistent with different observations. So together with these parametrizations, using present observational data, we cover a broad class of dark energy models[2] throughout the evolution of the Universe. Finally, let us emphasize that while the CPL parametrization was proposed as a phenomenological form for the equation of state of dark energy, both the SS and GCG parametrizations were obtained from a specific field theory Lagrangian under certain conditions [11,25].

III. METHODOLOGY

In this paper we put constraints on the late time evolution history of dark energy by contrasting multiple dark energy models with CMB and low redshift observations. For CMB we have used the recent Planck $C_\ell^{\rm TT}$ data. As Planck has not yet released the observed polarization data, we have used WMAP-9 [33] low-ℓ (2–23) polarization data (WP) for completeness, as has also been used in Planck analysis. In different frequency channels Planck has detected the CMB sky in much smaller scales ($\ell=2500$) compared to WMAP. Planck has published two likelihood estimators [20], namely, the low-ℓ (2–49) likelihood that is estimated by COMMANDER and the high-ℓ (50–2500) that is estimated by CAMSPEC, for four different frequency channels. At small scales, the foreground effects are dominant, and there are 14 nuisance parameters [20,34] corresponding to the foreground effects in different frequency channels along with the calibrations. For our analysis with CMB data, we have always marginalized over these nuisance parameters. The Planck baseline cosmological model is described by the six cosmological parameters: $\Omega_{\rm b}h^2$, $\Omega_{\rm CDM}h^2$, θ, τ, $A_{\rm S}$, and $n_{\rm S}$. The first four parameters describe the background where $\Omega_{\rm b}$ and $\Omega_{\rm CDM}$ represent the baryon and the cold dark matter density and h represents the Hubble parameter. θ is the ratio of the sound horizon to the angular diameter distance at decoupling, and τ is the reionization optical depth. $A_{\rm S}$ and $n_{\rm S}$ describe the amplitude and the spectral index of the primordial perturbation that we assume to be of the power-law form. Finally, for the CPL and GCG model we have two additional parameters, and for the SS model we have one additional parameter.

For non-CMB data, we have used Supernovae data, BAO data, and data from the HST. For Supernovae data we have used the recent Union 2.1 compilation [35] with 580 supernovae within redshifts $\sim 0.015-1.4$. We have used the covariance matrix of the Union 2.1 compilation which includes systematic errors. For the BAO we have used four data sets, namely the six-degree field galaxy survey [36], SDSS DR7 [37] and BOSS DR9 measurements [38], and the data from the WiggleZ survey [39]. We confront the theoretical model with the distance ratio $[d_z=r_s(z_{\rm drag})/D_{\rm V}(z)]$ measured by the particular surveys (and with the functions of d_z), where $z_{\rm drag}$ is the particular redshift where the baryon-drag optical depth becomes unity and $r_s(z_{\rm drag})$ is the comoving sound horizon at that redshift. $D_{\rm V}(z)$ is related to the angular diameter distance and the Hubble parameter at redshift z. For BAO we get constraints from six data points, of which three come from the WiggleZ survey at three different redshifts ($z=0.44, 0.6, 0.73$) and the other three come from the two SDSS measurements such as SDSS DR7: $z=0.35$; SDSS DR9: $z=0.57$; and a 6DF: $z=0.106$. We have also used the HST data [40], which uses the nearby Type-Ia Supernova data with Cepheid calibrations to constrain the value of H_0.

To study the inhomogeneous universe in a general covariance formalism, one has to take into account the dark energy perturbation together with the perturbation in the baryonic as well as dark matter sector. But on small scales, due to very small mass ($\sim 10^{-33}$ eV), the effect of dark energy perturbation is negligible and one can always assume dark energy to be a smooth component. On horizon scales, the dark energy perturbation can play an important role; but it is also known that on these scales cosmological measurements are strongly affected by cosmic variance. Hence in general dark energy perturbation does not play a major role in parameter estimation through CMB

[1] We shall demonstrate this fact in Section IV.

[2] Theoretically local inhomogeneities can also produce apparent phantom behavior of dark energy [32] that is highly localized in time. However, our analysis allows relatively smooth behavior of dark energy, and sharp changes are beyond the scope of this analysis.

TABLE I. Best fit $\chi^2_{\rm best\,fit}$ obtained for different models upon comparing against CMB + non-CMB data sets. The breakdown of the $\chi^2_{\rm best\,fit}$ for individual data are also provided. To obtain the best fit we have used Powell's BOBYQA method of iterative minimization.

Data	ΛCDM	CPL	SS	GCG
Planck (low-ℓ + high-ℓ)	7789.0	7787.4	7788.1	7789.0
WMAP-9 low-ℓ polarization	2014.4	2014.436	2014.455	2014.383
BAO: SDSS DR7	0.410	0.073	0.265	0.451
BAO: SDSS DR9	0.826	0.793	0.677	0.777
BAO: 6DF	0.058	0.382	0.210	0.052
BAO: WiggleZ	0.020	0.069	0.033	0.019
SN: Union 2.1	545.127	546.1	545.675	545.131
HST	5.090	2.088	2.997	5.189
Total	10355.0	10351.4	10352.4	10355.0

measurement. (It never plays any role for the background expansion.) To get a meaningful constraint on the dark energy perturbation, one needs to cross-correlate the large scale CMB measurement with those from large scale structures [41].

Nevertheless, to have a complete analysis, we consider the dark energy perturbation in our analysis [42]. The parameter that distinguishes different dark energy perturbation is the sound speed through the dark energy component, c_s^2, which is the ratio between the pressure and the energy density perturbation for the dark energy. For dark energy, modeled with a simple canonical scalar field, $c_s^2 = 1$.

In our study, we do not consider any particular dark energy model. Rather we consider different parametrizations for the dark energy equation of state that represent a broad class of dark energy behavior. This has been discussed in detail in Section II. In particular, for GCG parametrization, we should emphasize that this does not represent the original GCG model for dark matter-dark energy unification (where c_s^2 can have different values for different α and plays a major role); rather it represents the scalar field models in general, giving the thawing and the freezing behavior for the appropriate limit of parameter α. This is also true for the other sets of parametrization that represent different quintessence behavior that is considered in literature. Therefore, we fix $c_s^2 = 1$ in our subsequent calculations while considering dark energy perturbation. We again want to mention that even if we do not include the dark energy perturbation in our analysis, the conclusions will not change much.

We have used the publicly available cosmological Boltzmann code CAMB [43,44] to calculate the power spectrum for CMB and different observables for non-CMB observations, and for the Markov chain Monte Carlo (MCMC) analysis we have used the CosmoMC [45,46]. Throughout our analysis we have fixed the number of relativistic species to be $N_{\rm eff} = 3.046$.

IV. RESULTS

We start this section by showing, in Table I, the best-fit total χ^2 ($\chi^2_{\rm best\,fit}$) values for cosmological models with different dark energy parametrizations. In obtaining the best fits, we have used Powell's BOBYQA method of iterative minimization [47], and the $\chi^2_{\rm best\,fit}$ quoted are obtained from the joint analysis with CMB and all non-CMB data described in the previous section. The $\chi^2_{\rm best\,fit}$ are actually the minimum values obtained for the sums of χ^2 calculated for different data sets.[3] We have also presented the breakdown of the $\chi^2_{\rm best\,fit}$ from various data sets to clarify the preference of any individual data set toward different dark energy models. Note that allowing phantom behavior (i.e., for both CPL and SS parametrizations) results in a marginally better fit to the complete data sets by a $\Delta\chi^2_{\rm best\,fit} \sim \mathcal{O}(2-4)$. The improvement from ΛCDM for the CPL model is 3.6 and for the SS model is 2.6. This improvement in $\chi^2_{\rm best\,fit}$ is, arguably, not large enough to justify the necessity to venture into the phantom regime. GCG parametrization, which is a nonphantom model, has similar $\chi^2_{\rm best\,fit}$ values as in ΛCDM although it contains two extra parameters. This shows that if we restrict ourselves to nonphantom models—*a strong theoretical prior*—it is hard to distinguish them from a ΛCDM behavior as the best-fit value is always close to a model with $w = -1$.

It is clear from Table I, where the total and the individual $\chi^2_{\rm best\,fit}$ are given, that the Supernova data marginally favor the concordance ΛCDM model as well as the nonphantom GCG model compared to the other two parametrizations. Planck data prefer lower H_0 for ΛCDM, which does not agree well with the H_0 from HST, and the fit to HST gets worse. However, CPL and SS models allowing a phantom equation of state fit the data from both CMB and HST better than the cosmological constant at their best fit values.

[3]However, note that for obtaining the marginalized likelihoods we do not use this information but perform a full MCMC analysis using CosmoMC.

TABLE II. The mean values and the 68.3% uncertainties for different cosmological parameters. CPL, SS, and GCG mark the dark energy parametrizations used. The parameters w_0 and w_a represent $-A$ and α for the GCG model and have been indicated in the table. For each parameter the first, second, and last rows indicate the results from the analysis with CMB, CMB + non-CMB, and non-CMB data sets, respectively.

		CPL	SS	GCG
$\Omega_b h^2$	CMB	0.0221 ± 0.00028	0.0221 ± 0.00026	0.022 ± 0.00028
	CMB + non-CMB	0.022 ± 0.00026	$0.0221^{+0.00026}_{-0.00024}$	0.0223 ± 0.00024
	Non-CMB	$0.027^{+0.004}_{-0.005}$	$0.028^{+0.004}_{-0.006}$	0.029 ± 0.005
$\Omega_{CDM} h^2$	CMB	0.1196 ± 0.0027	0.1198 ± 0.0026	$0.1199^{+0.0026}_{-0.0028}$
	CMB + non-CMB	0.1209 ± 0.0023	0.1192 ± 0.0018	0.117 ± 0.0015
	Non-CMB	$0.126^{+0.014}_{-0.017}$	$0.128^{+0.014}_{-0.018}$	$0.127^{+0.015}_{-0.018}$
100θ	CMB	1.041 ± 0.0006	1.041 ± 0.0006	1.041 ± 0.0006
	CMB + non-CMB	1.041 ± 0.0006	1.041 ± 0.00056	1.042 ± 0.00056
	Non-CMB	1.042 ± 0.023	1.048 ± 0.022	$1.05^{+0.019}_{-0.027}$
τ	CMB	$0.09^{+0.012}_{-0.014}$	$0.09^{+0.012}_{-0.015}$	$0.09^{+0.013}_{-0.014}$
	CMB + non-CMB	$0.087^{+0.012}_{-0.014}$	0.091 ± 0.013	0.094 ± 0.014
	Non-CMB	...	...	...
$w_0[-A]$	CMB	$-1.13^{+0.37}_{-0.66}$	$-1.31^{+0.19}_{\text{unbounded}}$	$-0.827^{+0.06}_{\text{non-phantom prior cut}}$
	CMB + non-CMB	$-1.005^{+0.15}_{-0.17}$	$-1.14^{+0.08}_{-0.09}$	$-0.957^{+0.007}_{\text{non-phantom prior cut}}$
	Non-CMB	$-0.995^{+0.23}_{-0.27}$	-1.02 ± 0.12	$-0.92^{+0.018}_{\text{non-phantom prior cut}}$
$w_a[\alpha]$	CMB	$-1.15^{+0.6}_{\text{unbounded}}$	...	$-1.97^{+0.32}_{\text{unbounded}}$
	CMB + non-CMB	$-0.48^{+0.77}_{-0.54}$	...	$-2.0^{+0.29}_{\text{unbounded}}$
	Non-CMB	$-0.5^{+1.64}_{-0.94}$	...	$-1.49^{+0.4}_{\text{unbounded}}$
n_S	CMB	0.9607 ± 0.007	0.9603 ± 0.007	$0.9603 \pm +0.00073$
	CMB + non-CMB	$0.9579^{+0.0063}_{-0.0066}$	$0.9619^{+0.0059}_{-0.0057}$	$0.9669^{+0.00056}_{-0.00059}$
	Non-CMB	...	...	...
$\ln[10^{10} A_S]$	CMB	$3.089^{+0.023}_{-0.027}$	$3.089^{+0.023}_{-0.028}$	3.09 ± 0.025
	CMB + non-CMB	$3.087^{+0.024}_{-0.026}$	3.091 ± 0.025	3.092 ± 0.026
	Non-CMB	...	...	...
Ω_m	CMB	$0.239^{+0.028}_{-0.099}$	$0.27^{+0.04}_{-0.1}$	$0.344^{+0.022}_{-0.032}$
	CMB + non-CMB	$0.291^{+0.011}_{-0.013}$	$0.288^{+0.012}_{-0.013}$	$0.304^{+0.009}_{-0.011}$
	Non-CMB	0.29 ± 0.024	$0.298^{+0.02}_{-0.026}$	$0.3^{+0.021}_{-0.024}$
H_0	CMB	$80^{+17.8}_{-7.8}$	$74.8^{+13.3}_{-9.8}$	$64.6^{+2.61}_{-1.91}$
	CMB + non-CMB	70.26 ± 1.4	70.3 ± 1.4	$67.9^{+0.9}_{-0.7}$
	Non-CMB	72.68 ± 2.2	72.67 ± 2.15	72.4 ± 2.16

A direct upshot of these phantom equations of state that fits the CMB data better than the ΛCDM model is that it comes with a higher value of H_0 that in turn agrees with the HST data better too. However, for the same choice of best fit parameter values they do not provide similar improvement in $\chi^2_{\text{best fit}}$ for Supernovae data. This indicates that SN data favor the equations of state closer to the cosmological constant. The breakdown of $\chi^2_{\text{best fit}}$ points to the tantalizing possibility that different data sets, which effectively probe different epochs in the history of our Universe, prefer different kinds of dark energy behaviors. The improvement in the total $\chi^2_{\text{best fit}}$ for the CPL and SS models over ΛCDM and GCG is driven by the ability to have a higher H_0 albeit along with the associated preference for phantom behavior. However, to be conclusive, one would need to evaluate the complete marginalized likelihood behavior for the different models with respect to the diverse data sets.

In Table II, we quote the mean values as well as the 68.3% errors bars for different parameters ($\Omega_b h^2$, $\Omega_{CDM} h^2$, θ, τ, n_S, A_S, w_0, w_a, and the derived matter content Ω_m and Hubble constant H_0). For each parameter, the first row contains results from CMB data sets, the second row contains the results when we combine high- and low-redshift data, and the last row provides the results from non-CMB data sets. Note that bounds on H_0 become considerably weak for CMB analysis alone when we allow a phantom equation of state through CPL and SS. In all the cases w_0 ($-A$ for GCG) is better constrained with non-CMB data compared to the CMB data alone since w_0 determines the behavior of the dark energy model at low redshift. However, w_a (α for GCG) is constrained better by CMB data sets for CPL and GCG as it determines the change in the dark energy equation of state throughout the expansion of the Universe. It is clear that CPL and SS allow

lower Ω_m and higher H_0, whereas the GCG allows higher Ω_m and lower H_0 consistently for all the analyses.[4] It should be noted that for the CPL model the mean value of H_0 for the analysis with CMB data sets comes out to be 80 and the 1σ uncertainty stretches the upper bound to 98. For the SS model the bound on the H_0 CMB *only* analysis is better than CPL since the model has one dark energy parameter and therefore is less degenerate.

It should be mentioned that the use of the BAO data tightens the constraints on the background parameters. In this context we performed our CMB + non-CMB analysis without BAO data as well. For the SS model we find the bounds on Ω_m and H_0 relax to $0.286^{+0.014}_{-0.015}$ and 70.44 ± 1.6, respectively. For the GCG model we find $\Omega_m = 0.3^{+0.013}_{-0.015}$ and $H_0 = 68.08 \pm 1.1$. Notice that though marginal, the addition of BAO data certainly help us to constrain the background parameter more precisely. For the CPL model too we find results similar to Planck analysis [34]. Since the six BAO data sets do not contribute much to the total likelihood, the mean values of the parameters do not change as expected. However, compared to CMB only data from Planck + WP we find significant improvement in constraints when we add BAO. For the CPL model CMB + BAO provides $\Omega_m = 0.307^{+0.041}_{-0.046}$ and $H_0 = 68.9^{+4.1}_{-5.65}$; for the SS model we find $\Omega_m = 0.283^{+0.028}_{-0.03}$ and $H_0 = 71.3^{+3.5}_{-3.3}$; and for GCG we find $\Omega_m = 0.32^{+0.013}_{-0.02}$ and $H_0 = 66.3^{+1.6}_{-1.12}$. If we compare the results for these two quantities from the CMB only analysis from Table II, we find that while CMB cannot put tight constraints on the Hubble parameter and the matter density due to degeneracies with the equation of state of dark energy, the addition of BAO data breaks the degeneracies and can provide tighter constraints on these parameters. Moreover, note that for the CPL and SS models, BAO drags matter density to a higher value and the Hubble parameter to a lower value compared to CMB only values. For the GCG model, we notice opposite behavior.

We now present the marginalized likelihoods of parameters for the different dark energy parametrizations. The one-dimensional marginalized likelihoods for equation of state parameters for different dark energy models are shown in Fig. 1. Interestingly, in CPL as well as SS parametrization, the CMB data from Planck drag the present value of the equation of state (w_0) toward higher phantom values,[5] whereas the non-CMB data bring it closer to the cosmological constant ($w_0 = -1$). For the combined data sets, we find that the mean w_0 comes close to the cosmological constant ($w = -1$) but still stays in the phantom region.

One can argue that there remains a moderate tension between CMB and non-CMB data, which questions the effectiveness of a joint analysis of CMB + non-CMB data together in the future. However, it is hard to pull out a decisive argument from these plots whether and to what extent the cosmological constant is consistent with the data. The GCG model suggests no tension in CMB and non-CMB data sets, and the cosmological constant ($A = 1$), which is our prior limit, is certainly well inside the marginalized likelihoods obtained from all combinations of the data sets. For a better understanding of the tension between the data sets, which till now seems to be due to phantom priors, we need to look at the two-dimensional (2D) marginalized contours of dark energy equation of state parameters.

In Fig. 2, we show the marginalized 2D contour plots in $w_0 - w_a$ and $A - \alpha$ parameter planes for CPL and GCG parametrizations, respectively. The CPL case confirms the results earlier obtained by the Planck collaborations.[6] It shows that the cosmological constant behavior ($w_0 = -1, w_a = 0$) is disallowed at more than 1σ confidence level. Moreover, the region $w_0 > -1$ and $w_a > 0$ is highly constrained even at the 3σ confidence level, showing that it is very unlikely that dark energy behaved in nonphantom manner at all epochs. For the 2σ confidence contour, we find that the area under the region containing a complete nonphantom history/total area ~ 0.002; i.e., the probability of a complete nonphantom history of dark energy is 0.2% out of the total probability at 95.5%. This certainly points to the fact that the combined data sets have a strong inclination toward a dark energy that goes through $w < -1$ at least once in the past.

For GCG parametrization (which is valid only for the nonphantom region), as seen in Fig. 2, from the relative shaded region below and above the $\alpha = -1$ horizontal line we find that the thawing behavior ($\alpha < -1$) is more probable than the freezing behavior ($\alpha > -1$) for dark energy. Note here that the parameter α is unconstrained in the thawing direction, i.e., from below. From Eq. (6) we argue that for negative α, $w(\text{today}) = -A$ and $w(\text{past}) \to -1$. For $\alpha \to -\infty$, the equation of state will start today at $-A$ and immediately reach the cosmological constant in the past. The GCG plot in Fig. 2 indicates the more negative α is allowed, the less $-A$ (or w_0) can be constrained. Since more negative α brings faster convergence to the cosmological constant, the role of the parameter $-A$ in the expansion history of the Universe becomes negligible, and the data sets are not sensitive to the change of the parameter. Moreover, we would like to highlight that CMB and non-CMB data, in this context of GCG models, qualitatively distinguish the equation of state of dark energy. For example, while the CMB data

[4]For analysis with non-CMB data sets GCG indicates a higher value of H_0

[5]Basically w_0 is unconstrained in the phantom direction (with CMB only) up to the prior range considered in our analysis.

[6]A tiny deviation from the Planck result is mainly due to the addition of all the non-CMB data together (UNION2.1 + BAO + HST) with the CMB data from Planck and WP in our analysis.

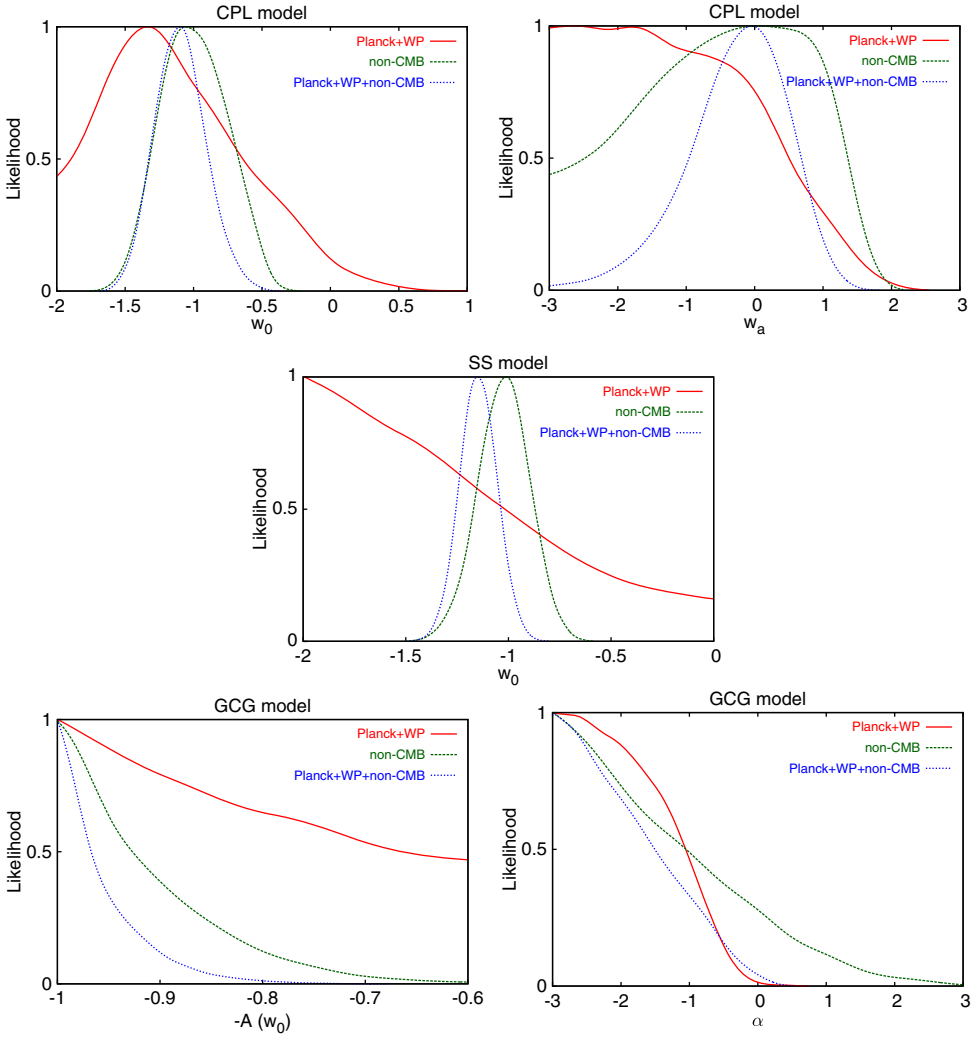

FIG. 1 (color online). The one-dimensional marginalized likelihoods for different parameters of the equation of state. The parametrizations are mentioned at the top of each plot. The color codes are for different analyses with different observational data and are described in the plot. Note here that for GCG, $-A$ corresponds to the equation of state of dark energy today, i.e., w_0.

constrain the value of α from above, non-CMB cannot provide a bound there. On the other hand, in constraining $-A$, the opposite happens (see the GCG plots in Fig. 1). Since non-CMB data (mainly SN) provide the most stringent constraints at the present epoch, it can constrain A much better than CMB data from Planck. However, SN data do not provide any information beyond $z \sim 1.4$ and therefore cannot constrain α as good as CMB data. Note that for $1 + \alpha > 0$ the denominator of Eq. (6) diverges at high redshift (small a) and makes $w \simeq 0$ (regardless of A), which is not supported by CMB data. This result clearly shows the sensitivity of two different probes toward two different parameters in the dark energy equation of state. Here, unlike the CPL and SS parametrizations, we can argue that CMB and non-CMB data may go through a joint analysis in order to obtain a tighter constraint on the dark energy equation of state. For both CPL and SS parametrization (that allow phantom behavior), the phantom-type equation of state is preferred for CMB + non-CMB data. Hence, irrespective of the equation of state parametrization with different numbers of parameters, phantom is preferred behavior for combined data. We should point out that allowing the phantom region in the parameter space brings in moderate tension between CMB and non-CMB (specifically SN data); note that there is no tension between them when we just concentrate on the nonphantom scenarios (as in GCG). At this point we would like to stress that if the two data sets do not have any systematic effects and since we claim that a reasonable theory should address different observational data to similar extent, our results highlight the interesting possibility of exploring and expanding theoretical ideas of dark energy. These new theories should fundamentally support an equation of state that evolves from a phantom nature at

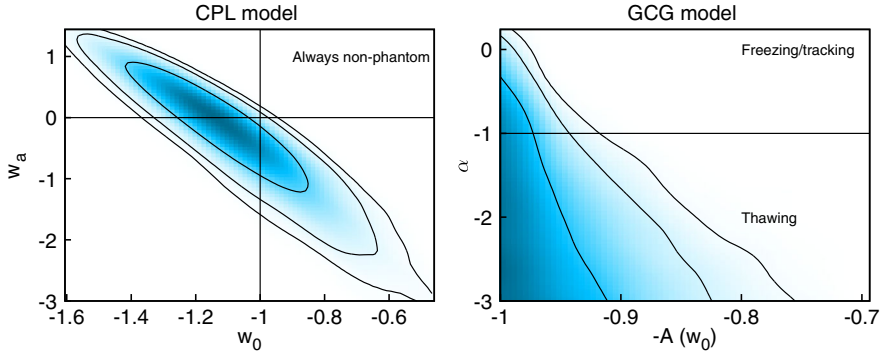

FIG. 2 (color online). Marginalized likelihoods in the $w_0 - w_a$ plane for CPL and the $A - \alpha$ plane for the GCG parametrization. Inward to outward the black bounding lines represent 68.3%, 95.5%, and 99.7% confidence contours, respectively. For CPL we have marked the cosmological constant with the intersection of two black lines, and for GCG we have marked the $1 + \alpha = 0$ line to distinguish between the freezing and thawing regions. Note here that for GCG, $-A$ corresponds to the equation of state of dark energy today, i.e., w_0.

high redshifts toward a cosmological constant behavior at low redshifts (as our results indicates).

Next, we analyze 2D confidence regions for other cosmological parameters. In Fig. 3, we show the confidence contours in the $w_0 - H_0$ plane for all three dark energy parametrizations. For the GCG model w_0 is defined as $-A$. The Planck best-fit measurements for H_0 for a concordance ΛCDM model is shown by the horizontal red line. The vertical black line represents the cosmological constant. In Fig. 4, we show the confidence contours in the $\Omega_m - H_0$ parameter plane for all three parametrizations; the red lines show the best-fit values for Ω_m and H_0 as measured by Planck for a concordance ΛCDM model. Our main aim is to address the issue of phantom behavior of the dark energy, i.e., whether it is allowed; and, if allowed, to what extend does it affect the constraints on other cosmological parameters?

Figures 3 and 4 show that if we allow a phantom equation of state (i.e., for CPL and SS parametrizations), the best fit cosmology shifts to a higher value of H_0 and a lower value of Ω_m. This shift leaves the base ΛCDM values measured by Planck outside the 2σ (95.5%) confidence limit (C.L.) for dark energy models captured by the CPL parametrization and at the border of the 2σ contour in case of SS parametrized models. However, for dark energy models described by the GCG parametrization—which does not allow phantom models—the Planck ΛCDM values are at the border of the 1σ C.L. To summarize, Planck measurements of high Ω_m and low H_0 values for the ΛCDM model are consistent with measurements of these two parameters using both CMB + non-CMB data *if* we restrict ourselves only to nonphantom models like GCG.

The behaviors of the equation of state as a function of redshift at 1σ and 2σ confidence levels, for the three parametrizations, are shown in Fig. 5. Below we point out the importance of this figure.

(A) The CPL parametrization (left panel in Fig. 5) prefers the dark energy equation of state to be phantom at more than the 1σ level beyond $z > 0.2$. Only at $z < 0.2$, we get the $w = -1$ line within the 1σ bound. In this parametrization, the mean dark energy equation of state starts as a cosmological constant at only $z = 0$ and quickly deviates from it to become phantomlike as redshift

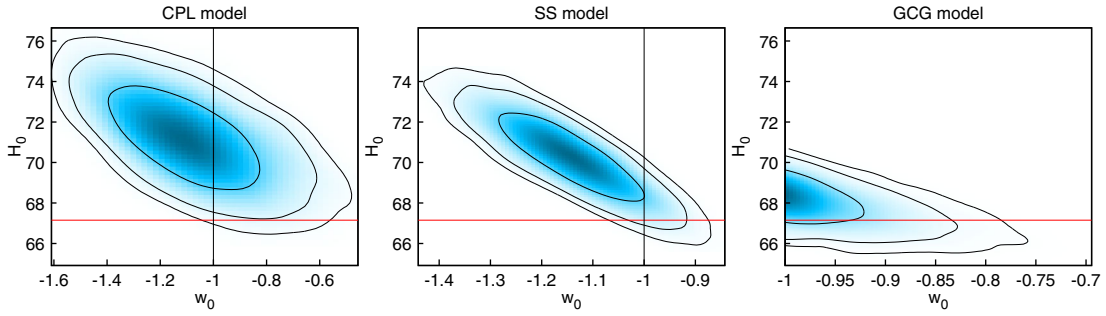

FIG. 3 (color online). Marginalized likelihoods in $w_0 - H_0$ parameter plane for CPL (left), SS (middle), and GCG (right) parametrizations. The red horizontal lines represent the best-fit value for H_0 obtained from Planck for ΛCDM case. Inward to outward the black bounding lines represent 68.3%, 95.5%, and 99.7% confidence contours, respectively.

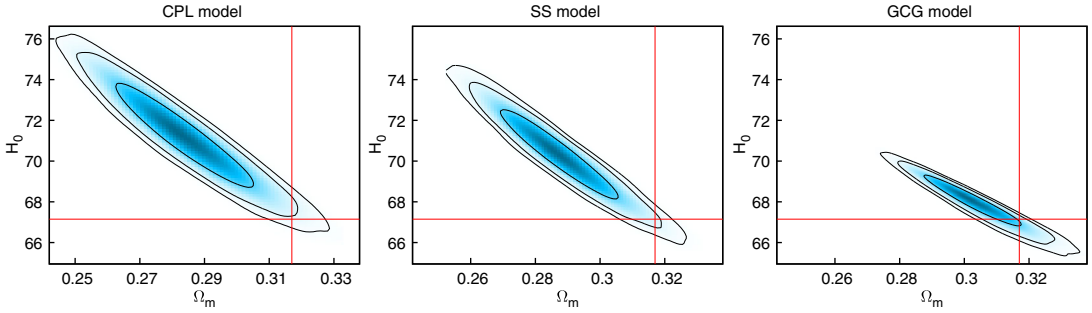

FIG. 4 (color online). Marginalized likelihoods in $\Omega_m - H_0$ parameter plane for CPL (left), SS (middle), and GCG (right) parametrizations. The red lines represent the best-fit values for H_0 and Ω_m obtained from Planck for ΛCDM model. Inward to outward the black bounding lines represent 68.3%, 95.5%, and 99.7% confidence contours, respectively.

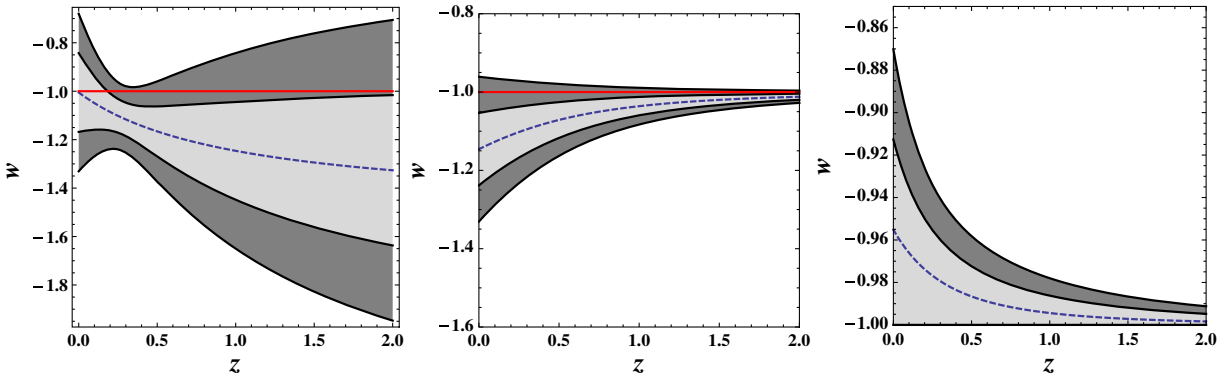

FIG. 5 (color online). Behavior of equation of state w as a function of redshift z for CPL (left), SS (middle), and GCG (right) parametrization for 68.3% and 95.5% confidence levels. The red solid and the blue dashed lines correspond to $w = -1$ and the mean w, respectively.

increases. w is best constrained at roughly around $z \sim 0.3$. Note that dark energy with $w \geq -1$ lies outside the inner grey region (1σ) in the range ($0.2 < z < 2$). Moreover, the equation of state parameters have an extremely small area to have $w \geq -1$ around $z \simeq 0.3$ and still be inside the 2σ band. This behavior of the equation of state is consistent with what we observe in the $w_0 - w_a$ confidence plane as discussed earlier. To summarize, w is consistent with ΛCDM only around $z = 0$ but becomes increasingly phantomlike with increasing redshift.[7]

(B) It is apparent that SS parametrization (middle panel in Fig. 5) constrains the equation of state to evolve very closely to $w = -1$; the 1σ region for w is always less than but within ∼5% to the cosmological constant at all epochs. This is expected as this parametrization represents thawing class scalar field models with small deviations from the cosmological constant. Hence, though the nonphantom behavior is not allowed at 1σ confidence level, at 2σ, w is consistent with the cosmological constant. Note that the mean w is always phantom and can provide reasonable deviation from cosmological constant behavior at the present epoch.

It is easy to understand the difference in the behavior of w for CPL and SS parametrizations. SS parametrization is designed to follow $w = -1$ in the early epoch and has flexibilities only at low redshifts. CPL, on the other hand, can allow more scenarios with one more degree of freedom. The important similarity between them is both the solutions permit a larger area in the phantom region. Note that the mean w from SS is allowed within the CPL 1σ bounds. The tighter constraints on w for the SS model at high redshift also reflects the inability of the SS model to depart from $w = -1$ at early epochs.

(C) The mean equation of state for the GCG parametrization (right panel in Fig. 5) shows that $w \approx -0.96$ at the present epoch and reaches close to $w = -1$ at high redshifts. The error bands clearly point to a preference toward the thawer class of models and hence provides an important constraint for scalar field models for dark energy. For this class

[7]Similar conclusions about the phantom behavior of dark energy has been recently reported by the Pan-STARRS1 survey [48].

of models, in the entire redshift range, the deviation of w from a cosmological constant is far less than what is found for the other two models.

From Fig. 5, the overall picture that emerges is the following: if one allows phantom behavior, early dark energy is very close to the cosmological constant (thawer type); in the recent past there is possible phantom crossing. Provided that CMB and non-CMB joint analysis does not impose systematic errors as has been discussed before, *our results can therefore be thought of as an invitation to construct models of dark energy that lead to phantom behavior*, at least at the scales probed by the Planck and non-CMB observations. In the nonphantom scenarios, thawer models are preferred and the dark energy equation of state increases toward higher values in the future resulting in the Universe decelerating again.

V. CONCLUSIONS

The post-Planck era has seen cosmological parameters best constrained till date using a CMB and a host of non-CMB measurements. This raises the possibility of precision determination of the nature of dark energy. In this paper we do a detailed investigation with such an aim in mind.[8] Currently, almost all the cosmological constraints on dark energy are based on a single parametrization, e.g., the CPL parametrization. However, theoretical models of dark energy abound in the literature, which leads to possibilities of having models that may not be fairly represented by such a parametrization. The question remains as to whether there are possible dark energy evolutions that one misses using the CPL parametrization.

To address the above-mentioned question we work with two other parametrizations, namely SS and GCG, apart from CPL. The SS model, which describes the dynamical equation of state with a single parameter, allows both phantom and nonphantom behavior and probes deviations close to the cosmological constant. The GCG model, on the other hand, represents only nonphantom models allowing *only* positive kinetic energies of an underlying scalar field model and provides a clear distinction between tracker and thawer models. Finally, while the CPL parametrization was proposed as a phenomenological form for the equation of state of dark energy, both the SS and GCG parametrizations were obtained from a specific field theory Lagrangian under certain conditions [11,25]. Hence, the three parametrizations together probe a significantly large parameter space for dark energy models.

Having the three parametrizations in hand, we use CMB and non-CMB data in a separate and combined analysis to look at dark energy behaviors. The main results of this study are summarized below:

(i) We find that *if* we allow phantom behavior of dark energy, irrespective of misgivings to its use due to the negative kinetic energy of scalar fields, the CMB data favor phantom behavior and the nonphantom equation of states stays at the edge of the 2σ region. On the other hand non-CMB data prefer nonphantom behavior for every parametrization considered. Once phantom behavior is allowed (i.e., in CPL and SS parametrizations), the combined CMB + non-CMB data allow regions such that the cosmological constant ($w = -1$) is pushed outside the 1σ confidence level contour. In this context, we refer to Table II where for the SS model the mean value of w_0 for non-CMB data sets ($w_0 = -1.02$) is more than 1σ away from the mean value obtained in the CMB-only analysis. Figure 1 also qualitatively indicates the same. This tension may be attributed to unknown systematics or the lack of a better theory/parametrization of the dark energy equation of state.

(ii) The GCG parametrization, which is theoretically constructed so as not to allow phantom models, shows consistency between CMB and non-CMB data although they have marginally worse likelihood than other parametrizations. It is found that the CMB and non-CMB observations are separately sensitive to the two parameters of the GCG parametrization and that the joint constraint is consistent with the cosmological constant. For these models, the cosmological parameters too are consistent with base Planck best-fit measurements.

(iii) From the results obtained with the three parametrizations, it comes out that for scalar field dark energy models, a thawing behavior is more probable than the freezing behavior. This is most clearly demonstrated in GCG models. Such an outcome is particularly interesting for quintessence model building in string theory. Currently the only quintessence model that has been constructed in string theory is the one given by Panda, Sumitomo, and Trivedi [28]. It was shown explicitly by them that this model does not allow a tracker behavior. Subsequently the thawer nature of this model was confirmed by [50].

(iv) The constraints on dark energy, coming out of a joint analysis of all available data, differ from model to model. Not only does the mean w depend on the parametrization of choice but also the error bar on the mean has different behavior. For SS and GCG parametrization, the nature of dark energy is best constrained at high redshifts; however, for the CPL parametrization the best constraints come in the redshift range of ≈ 0.2–0.3.

(v) Using the correlation between the equation of state parameters, we reconstruct the late time (i.e., $z < 2$) evolution of dark energy. For the SS models, the

[8] After we submitted our paper to the arXiv, a similar study and very similar conclusions were shown in [49].

$w = -1$ line stays outside the 1σ reconstructed band of the evolution history of dark energy for the entire redshift range. In the case of the CPL model, the $w = -1$ line stays outside the 1σ region for $z > 0.2$. From the ratio of the contour area occupied by complete nonphantom history and the overall equation of state allowed in CPL, we also note that a fine-tuning in w is required to have a complete nonphantom history and still be inside the 95.5% limit.

(vi) It has already been noticed in the cosmology community that the Planck measurement for the parameter H_0 for the ΛCDM model is in tension with the measurements from the HST. Note that as has been described in [51], the significance of this tension strongly depends on the analyses of the Cepheid calibration; and the use of the revised maser distance to NGC 4258 makes the obtained H_0 compatible with the Planck reported value. However, if we use the HST data from Riess *et al.* [40] we find that for SS and CPL parametrizations, where we allow phantom, a better fit to the data comes with a large value of H_0, which helps to agree better with the HST data. As has been described at the beginning of Sec. IV, in fact, the improvement in the total χ^2 for the CPL and SS model over ΛCDM and GCG is driven by the ability to have a higher H_0 albeit along with the associated preference for phantom behavior. However, in these parametrizations, the phantom effect drags the background cosmological parameter space (say, $\Omega_m - H_0$) in such a way that the corresponding best-fit base model and that from Planck becomes 2σ away from each other. For a pure nonphantom model (as in GCG), the above said parameters stay close to the values obtained in the ΛCDM model analysis. Hence, we demonstrated how to find the different model assumption bias cosmological parameter estimation. In this particular case, the extension to the phantom equation of state plays that crucial role.

Also, note that when we allow phantom behavior, the H_0 becomes highly degenerate with the dark energy equation of state in the case of CMB only measurements. Other parametrizations that allow nonphantom behaviors only do not exhibit similar behavior; the H_0 errors for CPL are ≈5 times larger compared to GCG for CMB only, even though both have the same number of degrees of freedom.

The conclusions drawn above, in the current work, come from a joint analysis of CMB and non-CMB data using different evolving dark energy models having different parametrizations of the equation of state of dark energy. In a detailed analysis of SNe data (along with other data sets), the PAN-STARRS1 survey [48] recently found hints for similar phantom behavior of dark energy, although using a constant equation of state. Their value of w is inconsistent with the cosmological constant at $> 2\sigma$ level (if used along with Planck data) or at $< 2\sigma$ (if used along with WMAP-9 data). Recently, in an arXiv submission [49] following our work, it was also reported that for data set Planck + HST + BAO + SNLS3 the ΛCDM model is just outside the 2σ confidence regime, while for the data set WMAP − 9 + HST + BAO + SNLS3 the ΛCDM model is 1σ away from the best fit. All these works complement each other.

A very important point, not adequately appreciated in the literature (and missed in the two papers [48,49] cited above), comes out in Fig. 5. This is the fact that *our constraints on w and hence the nature of dark energy that we infer from cosmological observation depends crucially on the choice of the underlying parametrization of the equation of state.* In fact, (any) deviation of w from a cosmological constant with redshift depends on the parametrization; whereas for the current available data, both SS and GCG infer dark energy being close to the cosmological constant at high redshift but "deviating from it in two different directions" when we approach the current epoch; on the other hand, CPL is close to the cosmological constant at the current epoch and deviates away at high z. Given this trichotomy, it is important to do nonparametric reconstruction of w for the total data set to infer the correct nature of dark energy without any priors on the form of w.

To summarize once again, we have performed one of the most comprehensive studies of the dark energy equation of state constraints from a joint analysis of Planck CMB data along with SNe, BAO, and H_0 data. A central result of our analysis is that if one allows for phantom behavior in the dark energy equation of state, the phantom region provides a better fit to the combined CMB and non-CMB data. This result motivates the construction of models of dark energy that lead to phantom behavior. This means violating the weak energy condition that cannot be possible with a single scalar field having a positive kinetic energy term. However, it is well known that in consistent theories of gravity, like string theory, the weak energy condition and also the null energy condition can be violated due to the presence of higher derivative corrections [52]. We leave it as an intriguing question for the reader as to whether such violations can be used to construct a model of dark energy that would fit the data better than, say, a positive cosmological constant.

ACKNOWLEDGMENTS

The authors would like to thank Sandip Trivedi for motivation, discussions, and support throughout the project. D. K. H. wishes to acknowledge support from the Korea Ministry of Education, Science and Technology, Gyeongsangbuk-Do and Pohang City for Independent Junior Research Groups at the Asia Pacific Center for Theoretical Physics. A. A. S. acknowledges the funding from SERC, Department of Science and Technology,

Government of India through the research Project No. SR/S2/HEP-43/2009. S. P. thanks ISI, Kolkata, for support through a research grant. The authors would like to thank Sandip Trivedi for motivation, discussions, and support throughout the project. We also acknowledge the use of publicly available CAMB and CosmoMC in our analysis. This project is part of the Dark Universe Initiative program.

[1] E. J. Copeland, M. Sami, and S. Tsujikawa, Int. J. Mod. Phys. D **15**, 1753 (2006); M. Li, X. D. Li, and S. Wang, Commun. Theor. Phys. **56**, 525 (2011); V. Sahni and A. A. Starobinsky, Int. J. Mod. Phys. D **09**, 373 (2000); S. M. Carroll, Living Rev. Relativity **4**, 1 (2001); P. J. E. Peebles and B. Ratra, Rev. Mod. Phys. **75**, 559 (2003); T. Padmanabhan, Phys. Rep. **380**, 235 (2003).

[2] A. G. Riess *et al.*, Astron. J. **116**, 1009 (1998); Astrophys. J. **607**, 665 (2004); S. Perlmutter *et al.*, Astrophys. J. **517**, 565 (1999); J. L. Tonry *et al.*, Astrophys. J. **594**, 1 (2003); R. A. Knop *et al.*, Astrophys. J. **598**, 102 (2003); R. Amanullah *et al.*, Astrophys. J. **716**, 712 (2010); N. Suzuki *et al.*, Astrophysics J. **746**, 85 (2012).

[3] E. Komatsu *et al.*, Astrophys. J. Suppl. Ser. **192**, 18 (2011).

[4] See http://www.sciops.esa.int/index.php?project=planck&page=Planck_Collaboration.

[5] D. Eisenstein, Astophys. J. **633**, 560 (2005).

[6] S. Kachru, R. Kallosh, A. D. Linde, J. M. Maldacena, L. P. McAllister, and S. P. Trivedi, J. Cosmol. Astropart. Phys. 10 (2003) 013.

[7] B. Ratra and P. J. E. Peebles, Phys. Rev. D **37**, 3406 (1988); M. S. Turner and M. White, Phys. Rev. D **56**, R4439 (1997); R. R. Caldwell, R. Dave, and P. J. Steinhardt, Phys. Rev. Lett. **80**, 1582 (1998); A. R. Liddle and R. J. Scherrer, Phys. Rev. D **59**, 023509 (1998); P. J. Steinhardt, L. Wang, and I. Zlatev, Phys. Rev. D **59**, 123504 (1999); R. J. Scherrer and A. A. Sen, Phys. Rev. D **77**, 083515 (2008).

[8] C. Armendariz-Picon, T. Damour, and V. Mukhanov, Phys. Lett. B **458**, 209 (1999); J. Garriga and V. F. Mukhanov, Phys. Lett. B **458**, 219 (1999); T. Chiba, T. Okabe, and M. Yamaguchi, Phys. Rev. D **62**, 023511 (2000); C. Armendariz-Picon, V. Mukhanov, and P. J. Steinhardt, Phys. Rev. Lett. **85**, 4438 (2000); Phys. Rev. D **63**, 103510 (2001); T. Chiba, Phys. Rev. D **66**, 063514 (2002); L. P. Chimento and A. Feinstein, Mod. Phys. Lett. A **19**, 761 (2004); L. P. Chimento, Phys. Rev. D **69**, 123517 (2004); R. J. Scherrer, Phys. Rev. Lett. **93**, 011301 (2004).

[9] R. R. Caldwell, Phys. Lett. B **545**, 23 (2002).

[10] J. S. Bagla, H. K. Jassal, and T. Padmanabhan, Phys. Rev. D **67**, 063504 (2003); A. A. Sen, J. Cosmol. Astropart. Phys. 03 (2006) 010.

[11] M. C. Bento, O. Bertolami, and A. A. Sen, Phys. Rev. D **66**, 043507 (2002).

[12] A. A. Sen and R. J. Scherrer, Phys. Rev. D **72**, 063511 (2005).

[13] M. Chevallier and D. Polarski, Int. J. Mod. Phys. D **10**, 213 (2001).

[14] E. V. Linder, Phys. Rev. Lett. **90**, 091301 (2003).

[15] R. J. Scherrer and A. A. Sen, Phys. Rev. D **77**, 083515 (2008).

[16] M. C. Bento, O. Bertolami, and A. A. Sen, Gen. Relativ. Gravit. **35**, 2063 (2003).

[17] M. C. Bento, O. Bertolami, and A. A. Sen, arXiv:astro-ph/0210375.

[18] M. C. Bento, O. Bertolami, and A. A. Sen, Phys. Rev. D **67**, 063003 (2003).

[19] M. C. Bento, O. Bertolami, and A. A. Sen, Phys. Lett. B **575**, 172 (2003).

[20] P. A. R. Ade *et al.* (Planck Collaboration), Astron. Astrophys. **571**, A15 (2014).

[21] A. Shafieloo, Mon. Not. R. Astron. Soc. **380**, 1573 (2007).

[22] A. Shafieloo, J. Cosmol. Astropart. Phys. 08 (2012) 002.

[23] A. Shafieloo, V. Sahni, and A. A. Starobinsky, Phys. Rev. D **80**, 101301(R) (2009).

[24] J. Q. Xia, H. Li, and X. Zhang, Phys. Rev. D **88**, 063501 (2013); V. Pettorino, Phys. Rev. D **88**, 063519 (2013); V. Salvatelli, A. Marchini, L. Lopez-Honorez, and O. Mena, Phys. Rev. D **88**, 023531 (2013); E. Macaulay, I. K. Wehus, and H. K. Eriksen, arXiv:1303.6583; C. Cheng and Q.-G. Huang, Phys. Rev. D **89**, 043003 (2014).

[25] R. J. Scherrer and A. A. Sen, Phys. Rev. D **78**, 067303 (2008).

[26] A. Ali, M. Sami, and A. A. Sen, Phys. Rev. D **79**, 123501 (2009).

[27] E. Bergshoeff, M. de Roo, T. de Wit, E. Eyras, and S. Panda, J. High Energy Phys. 05 (2000) 009.

[28] S. Panda, Y. Sumitomo, and S. P. Trivedi, Phys. Rev. D **83**, 083506 (2011).

[29] A. Y. Kamenshchik, U. Moschella, and V. Pasquier, Phys. Lett. B **511**, 265 (2001).

[30] N. Bilic, G. B. Tupper, and R. D. Viollier, Phys. Lett. B **535**, 17 (2002).

[31] S. Thakur, A. Nautiyal, A. A. Sen, and T. R. Seshadri, Mon. Not. R. Astron. Soc. **427**, 988 (2012).

[32] A. E. Romano, M. Sasaki, and A. A. Starobinsky, Eur. Phys. J. C **72**, 2242 (2012).

[33] G. Hinshaw *et al.* (WMAP Collaboration), Astrophys. J. Suppl. Ser. **208**, 19 (2013).

[34] P. A. R. Ade *et al.* (Planck Collaboration), Astron. Astrophys. **571**, A16 (2014).

[35] N. Suzuki *et al.*, Astrophys. J. **746**, 85 (2012).

[36] F. Beutler, C. Blake, M. Colless, D. Heath Jones, L. Staveley-Smith, L. Campbell, Q. Parker, W. Saunders, and F. Watson, Mon. Not. R. Astron. Soc. **416**, 3017 (2011).

[37] W. J. Percival *et al.* (SDSS Collaboration), Mon. Not. R. Astron. Soc. **401**, 2148 (2010).

[38] L. Anderson *et al.*, Mon. Not. R. Astron. Soc. **427**, 3435 (2012).

[39] C. Blake *et al.*, Mon. Not. R. Astron. Soc. **418**, 1707 (2011).

[40] A. G. Riess, L. Macri, S. Casertano, H. Lampeitl, H. C. Ferguson, A. V. Filippenko, S. W. Jha, W. Li, and R. Chornock, Astrophys. J. **730**, 119 (2011); **732**, 129(E) (2011).
[41] P. S. Corasaniti, T. Giannantonio, and A. Melchiorri, Phys. Rev. D **71**, 123521 (2005).
[42] W. Fang, W. Hu, and A. Lewis, Phys. Rev. D **78**, 087303 (2008).
[43] A. Lewis, A. Challinor, and A. Lasenby, Astrophys. J. **538**, 473 (2000).
[44] See http://camb.info/.
[45] A. Lewis and S. Bridle, Phys. Rev. D **66**, 103511 (2002).
[46] See http://cosmologist.info/cosmomc/.
[47] M. J. D. Powell, Report No. NA2009/06, University of Cambridge, Cambridge, 2009.
[48] A. Rest *et al.*, Astrophys. J. **795**, 44 (2014).
[49] B. Novosyadlyj, O. Sergijenko, R. Durrer, and V. Pelykh, J. Cosmol. Astropart. Phys. 05 (2014) 030.
[50] G. Gupta, S. Panda, and A. A. Sen, Phys. Rev. D **85**, 023501 (2012); S. Kumar, S. Panda, and A. A. Sen, Classical Quantum Gravity **30**, 155011 (2013).
[51] G. Efstathiou, Mon. Not. R. Astron. Soc. **440**, 1138 (2014).
[52] P. Creminelli, G. D'Amico, J. Norena, and F. Vernizzi, J. Cosmol. Astropart. Phys. 02 (2009) 018.